Journal of Materials Science and Chemical Engineering, 2026, 14(3), 107-118
https://www.scirp.org/journal/msce
ISSN Online: 2327-6053
ISSN Print: 2327-6045

# Air-Assisted Melt Centrifugal Electrospinning of PET: Process Control, Structural Evolution, and Performance

**Hao Ding, Yuyang Wang**

Research Center of Fluid Machinery Engineering and Technology, Jiangsu University, Zhenjiang, China
Email: dinghao0323@163.com

**How to cite this paper:** Ding, H. and Wang, Y.Y. (2026) Air-Assisted Melt Centrifugal Electrospinning of PET: Process Control, Structural Evolution, and Performance. *Journal of Materials Science and Chemical Engineering*, **14**, 107-118.
https://doi.org/10.4236/msce.2026.143008

**Received:** January 14, 2026
**Accepted:** March 24, 2026
**Published:** March 27, 2026



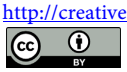



## Abstract

Polyethylene terephthalate (PET) micro/nanofibers are pivotal for advanced textiles and filtration materials, yet their industrial production is currently constrained by the environmental toxicity of solution electrospinning and the coarse fiber diameters typical of conventional melt spinning. Air-Assisted Melt Centrifugal Electrospinning (A-MCES) has emerged as a transformative, solvent-free technique that overcomes these limitations by integrating centrifugal inertia, electrostatic forces, and high-velocity aerodynamic shear. This review provides a comprehensive analysis of the state-of-the-art in A-MCES of PET, specifically focusing on process control, structural evolution, and material performance. We systematically elucidate the critical role of airflow in regulating the thermal history of the melt jet to achieve sub-micron attenuation. Key processing parameters—ranging from intrinsic viscosity to nozzle geometry—are discussed in the context of process optimization. Furthermore, the structure-property relationships are critically examined, revealing how the unique interplay between rapid aerodynamic cooling and high-strain elongation promotes stress-induced crystallization (SIC), which is decisive for mechanical strength. Finally, the review highlights the applications of A-MCES fibers in high-efficiency filtration and biomedical scaffolds, concluding with a perspective on overcoming current challenges related to energy efficiency and uniformity.

## Keywords

Air-Assisted Melt Centrifugal Electrospinning, Polyethylene Terephthalate (PET), Stress-Induced Crystallization, Green Manufacturing, Nanofibers, Structure-Property Relationship

## 1. Introduction

Polyethylene terephthalate (PET) microfibers and nanofibers have garnered significant attention in recent decades due to their superior mechanical properties, thermal stability, and recyclability. These materials are critical for high-performance applications ranging from industrial filtration and protective textiles to biomedical scaffolds. Traditionally, solution electrospinning has been the dominant method for fabricating continuous ultrafine fibers [1]. However, the reliance on toxic organic solvents (e.g., TFA, DCM) poses severe environmental risks, incurs high recovery costs, and limits the yield, thereby hindering industrial-scale production [2].

To address these limitations, melt electrospinning has emerged as a "green" and solvent-free alternative. Despite its eco-friendliness, conventional melt electrospinning faces inherent challenges: the high viscosity of polymer melts and the rapid solidification of the jet typically result in fibers with large diameters (often > 10 μm) and low production efficiency compared to solution-based processes [3]. Consequently, enhancing the drag force on the melt jet to achieve finer diameters while maintaining high throughput has become a focal point of research. The hybrid technique of Air-Assisted Melt Centrifugal Electrospinning (A-MCES) represents a synergistic approach that combines the thinning capability of the electric field, the high throughput of centrifugal force, and the strong shear stretching of airflow. In this multi-force field coupling, the centrifugal force provides a "pumping effect" to boost productivity, effectively overcoming the feed rate limitations of traditional methods [4]. Meanwhile, the high-velocity auxiliary airflow exerts a powerful drag force that exceeds the electric stress, driving the rapid attenuation of the fiber into the sub-micron scale [5].

While individual aspects of melt electrospinning and centrifugal spinning have been reviewed separately, a comprehensive understanding of the process optimization and structure-property relationships in the specific context of A-MCES of PET is still developing. This review aims to systematically summarize recent advances in A-MCES. We focus on elucidating the influence of key processing parameters on fiber morphology and establishing the critical link between the rapid cooling dynamics and the resulting microstructure, particularly stress-induced crystallization (SIC), which dictates the final mechanical performance [6].

## 2. Principles of A-MCES

### 2.1. Synergistic Mechanism of Multi-Physical Fields

The fundamental principle of A-MCES relies on the superposition of three distinct external forces acting on the polymer melt, each serving a specific function in the fiber formation process (**Figure 1**):

Centrifugal Force (Mass Ejection): High-speed rotation generates inertial forces that push the viscous PET melt through the spinneret orifices. Unlike traditional

electrospinning, where throughput is limited by the capillary feed rate, the centrifugal force provides a "pumping effect" that significantly enhances the mass flow rate. Sarkar, K. *et al.* demonstrated that the centrifugal inertia dominates the initial jet ejection, enabling the processing of high-viscosity melts that are typically difficult to spin using electric fields alone [7]. Aerodynamic Shear Force (Attenuation & Thermal Control): This is the critical component for refining fiber diameter in melt processes. A coaxial high-velocity airflow exerts a powerful drag force on the jet surface. Jin, M. *et al.* revealed that when using supersonic airflow (via Laval nozzles), the aerodynamic drag stress can exceed the electric stress by an order of magnitude, driving the rapid attenuation of the fiber from hundreds of micrometers to the sub-micron scale [8]. Furthermore, the hot airflow creates a localized thermal envelope, delaying the crystallization of PET and allowing for extended elongation time. Electrostatic Force (Dispersion): While the electric field contributes to stretching, its primary role in A-MCES is ensuring fiber separation. The Coulombic repulsion between the charged fibers prevents them from merging or agglomerating during flight. Li, Y. *et al.* emphasized that this electrostatic effect is also crucial for imparting electret properties to the fibers, which significantly enhances filtration efficiency by capturing fine particles via electrostatic attraction [9].

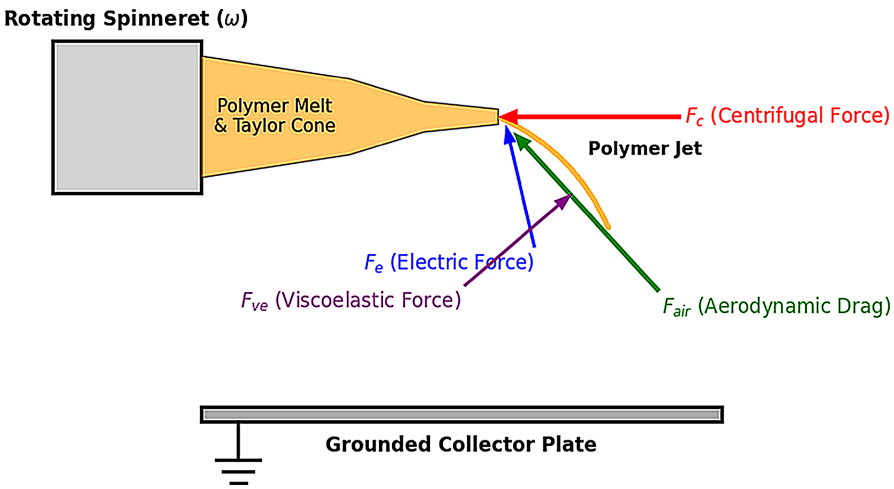


**Figure 1.** Schematic diagram of the A-MCES process illustrating the synergistic coupling of centrifugal force, electrostatic field, and aerodynamic shear. (Adapted from Jin, M. *et al.* [8]).

At the nozzle tip, the formation and attenuation of the polymer jet depend on a critical force balance. For the jet to be successfully ejected and stretched, the sum of the driving forces—namely, the aerodynamic drag (Fair), centrifugal force (Fc), and electrostatic force (Fe)—must overcome the resistive forces, which primarily consist of the melt's viscoelastic force (Fve) and surface tension (F):

$$\text{Fair} + \text{Fc} + \text{Fe} > \text{Fve} + \text{F}\gamma$$

In the A-MCES process, the high-velocity aerodynamic drag (Fair) plays the

decisive role in overcoming the high viscoelastic resistance (Fve) of the PET melt, which is typically the main bottleneck in conventional melt spinning.

### 2.2. Equipment Configuration

A typical A-MCES apparatus is engineered to handle high temperatures (>260˚C), high voltage, and high rotation speeds simultaneously (Figure 2).

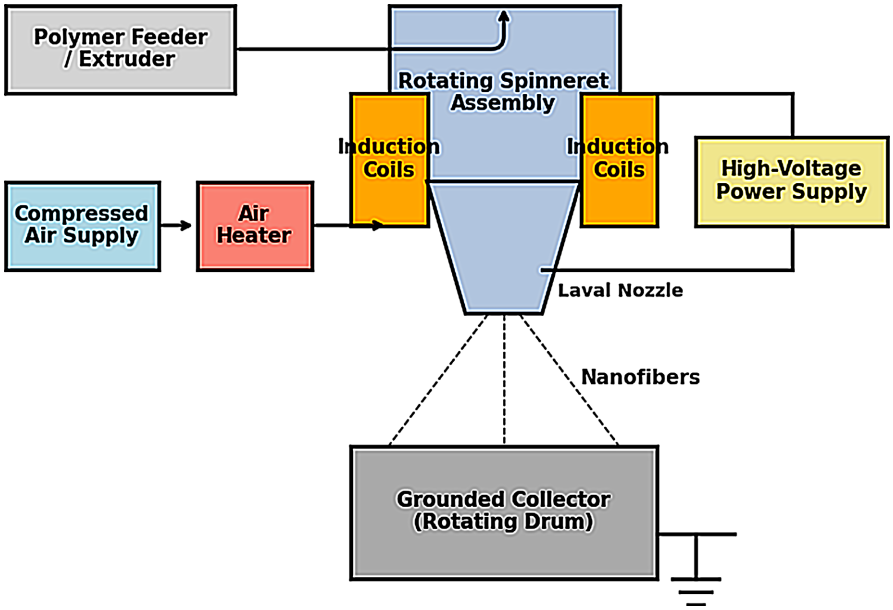


Figure 2. Configuration of the spinneret and Laval nozzle design for supersonic airflow acceleration. (Adapted from Jin, M. *et al.* [8]).

Spinneret and Nozzle Design: The core component is a conductive, rotating spinneret. Recent advancements have moved from simple annular gaps to Laval nozzles (convergent-divergent design). Research indicates that Laval nozzles can accelerate the airflow to supersonic speeds (Mach > 1), maximizing the kinetic energy transfer from the air to the polymer jet [10].

Heating and Collection: To maintain the PET melt at a precise temperature, high-frequency induction heating is often employed due to its rapid response and efficiency. For collection, a grounded drum or conveyor belt is placed at a specific working distance. Zander N. E. *et al.* highlighted that precise control of the collector temperature is critical to prevent secondary crystallization shrinkage of the deposited fibers, which ensures the dimensional stability of the final nonwoven mat [11].

## 3. Key Processing Parameters

The morphology and performance of A-MCES PET fibers are governed by a complex interplay of material properties and processing conditions. Optimizing these parameters is essential to achieve defect-free nanofibers with the desired diameter and crystallinity.

### 3.1. Intrinsic Viscosity (IV) and Molecular Weight

The intrinsic viscosity (IV) of the PET melt serves as a primary indicator of its molecular entanglement capability, which directly dictates spinnability.

High IV (>0.8 dL/g): Provides sufficient melt strength to sustain a continuous jet under high centrifugal and aerodynamic forces, preventing capillary breakup. However, excessive viscosity requires higher processing temperatures, which risks thermal degradation. Low IV (<0.6 dL/g): Often associated with recycled PET (r-PET). Due to chain scission during previous thermal histories, low-IV melts tend to form unstable jets, leading to "beads-on-string" defects. Awaja, F. and Pavel, D. demonstrated that while processing recycled PET requires careful viscosity management, it is feasible to produce uniform nanofibers from waste streams by optimizing the shear rate to compensate for lower molecular weights (**Figure 3**) [12].

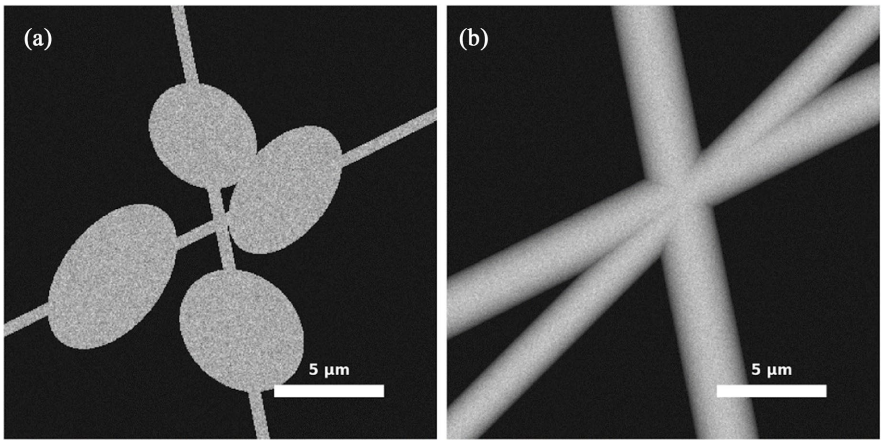


**Figure 3.** Scanning Electron Micrographs (SEM) showing the effect of melt viscosity on fiber morphology: (a) Low viscosity/r-PET leading to "beads-on-string" defects; (b) Optimal viscosity resulting in uniform and continuous nanofibers. (Based on Awaja, F. and Pavel, D. [12]).

Degradation Control: Dalton, P. D. *et al.* emphasized that thermal degradation during the melt process exponentially reduces IV, thereby compromising the mechanical integrity of the final fibers. Thus, residence time in the extruder must be strictly minimized [13].

### 3.2. Processing Temperature

Temperature control in A-MCES is twofold: the melt temperature and the ambient environmental temperature (air temperature). Melt Temperature: Must be maintained 20˚C - 40˚C above the melting point (Tm ≈ 255˚C) to ensure flowability. Greiner, A. and Wendorff, J. H. noted in their review that insufficient heating leads to nozzle clogging, while overheating causes polymer dripping and reduced molecular orientation [14].

Air Temperature: The temperature of the assisting airflow is a critical variable unique to this technique. Liu, C. *et al.* reported that using high-temperature airflow not only facilitates jet attenuation but can also induce a rough, porous surface structure on the fibers. This thermally induced phase separation (TIPS) effect sig-

nificantly enhances the specific surface area, making the fibers ideal for oil absorption applications [15].

Compared to conventional melt spinning, which has relatively slow cooling rates that allow polymer chains to relax, A-MCES utilizes the rapid expansion of high-velocity airflow to achieve ultra-fast cooling rates, often exceeding 1000˚C/s.

### 3.3. Airflow Pressure and Rotational Speed

The "Air-Centrifugal" coupling requires a delicate balance between aerodynamic pressure and rotational inertia. Airflow Pressure: Increasing the air pressure enhances the drag force, leading to finer fiber diameters. However, turbulence at supersonic speeds can cause fiber whipping and breakage if not controlled. Rotational Speed: Higher speeds increase the mass ejection rate (throughput). Reneker, D. H. and Yarin, A. L. investigated the optimization of these parameters for air filtration. They found that a synchronized increase in rotational speed and air pressure is necessary to maintain a hierarchical structure that efficiently captures PM2.5 particles while maintaining low air resistance (**Figure 4**) [16].

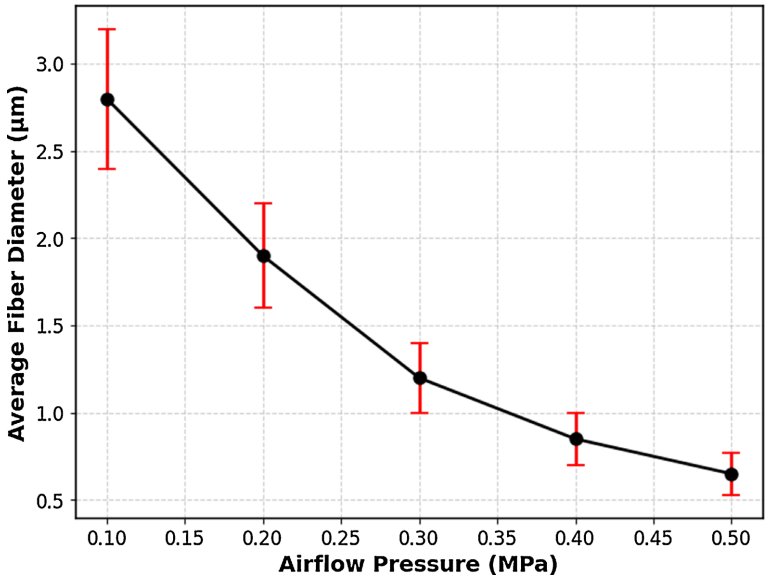


**Figure 4.** Effect of airflow pressure on average fiber diameter, showing a decreasing trend with increasing drag force. (Data trend adapted from Reneker, D. H. and Yarin, A. L. [16]).

## 4. Structure and Performance

The unique combination of high-temperature melting, rapid aerodynamic cooling, and supersonic stretching in A-MCES imparts distinct hierarchical structures to PET fibers. Understanding these structure-property relationships is crucial for tailoring fibers for specific applications.

### 4.1. Stress-Induced Crystallization (SIC)

Unlike solution electrospinning, where crystallization is largely solvent-driven, structure formation in A-MCES is dominated by the thermal history and stress

field [17]. PET is intrinsically a slow-crystallizing polymer; however, the ultra-high strain rates (>$10^3$ $s^{-1}$) provided by the high-velocity airflow significantly alter its crystallization kinetics. Perret, E. and Hufenus, R. investigated the structural evolution of PET under high-speed melt spinning conditions using Wide-Angle X-ray Diffraction (WAXD). They observed that the intense aerodynamic drag induces a transition from an amorphous state to a highly oriented mesomorphic phase, which subsequently acts as a precursor for rapid crystallization (**Figure 5**). This phenomenon, known as Stress-Induced Crystallization (SIC), results in fibers with high molecular orientation and superior mechanical modulus compared to those produced by quiescent crystallization [18].

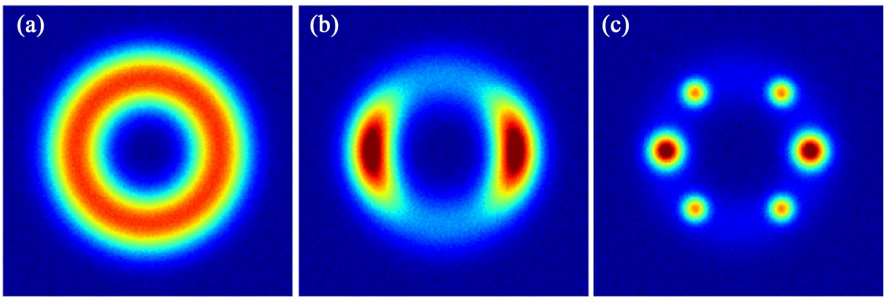


**Figure 5.** WAXD structural evolution (Simulated). (a) Low speed (Amorphous Halo); (b) Medium speed (Mesomorphic Arcs); (c) High speed (Crystalline Spots) showing Stress-Induced Crystallization (SIC). (Illustrating principles from Perret, E. and Hufenus, R. [18]).

This ultra-fast cooling rate effectively 'freezes' the highly oriented mesomorphic phase in place before the PET polymer chains have sufficient time to relax back into a random coil configuration, thereby locking in the stress-induced crystallization (SIC).

### 4.2. Surface Morphology and Wettability

While traditional melt-spun fibers typically exhibit smooth surfaces, A-MCES allows for the engineering of surface topography through environmental control. The rapid evaporation of moisture or the interplay between cooling rates and phase separation can induce nanoscale roughness on the fiber surface. Xue, J. *et al.* utilized this effect to fabricate PET nanofibrous membranes with a hierarchical rough structure. Their study demonstrated that these A-MCES fibers exhibited superhydrophobicity (water contact angle > 150˚) and superoleophilicity, making them highly effective for oil/water separation applications (**Figure 6**). The rough surface structure significantly increases the specific surface area, enhancing the adsorption capacity for oils and organic solvents [19].

### 4.3. Dimensional Stability in Scaffolds

For biomedical applications, the structural integrity of the fiber mat is as critical as individual fiber strength. A-MCES, particularly when adapted for Melt Electrospinning Writing (MEW), offers precise control over fiber placement and bond-

ing. Puguan, J. M. *et al.* explored the use of PCL/PET blends in tissue engineering. They found that the incorporation of PET segments via melt electrospinning improved the mechanical stiffness and dimensional stability of the scaffolds, preventing the shrinkage often observed in pure PCL scaffolds during cell culture. This structural reinforcement is attributed to the high melting point and stable crystalline domains of the PET microfibers formed during the process [20].

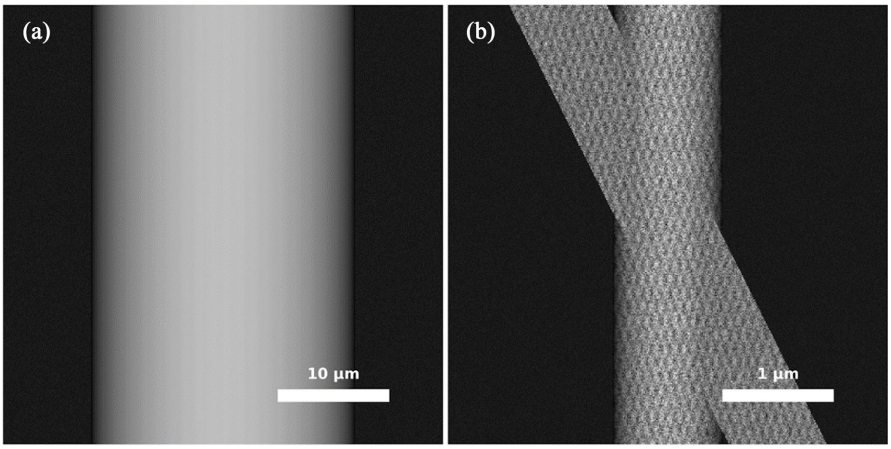


**Figure 6.** Scanning Electron Micrographs (SEM) of surface morphology comparison. (a) Conventional melt-spun fibers with smooth surfaces; (b) A-MCES nanofibers exhibiting hierarchical rough/porous surfaces for superhydrophobicity. (Based on Xue, J. *et al.* [19]).

## 5. Applications

Beyond the well-established applications in air filtration and biomedical scaffolds, the unique structural characteristics of A-MCES PET fibers—specifically their high specific surface area, porosity, and tortuous pore channels—have opened new avenues in acoustics, functional textiles, and energy storage.

### 5.1. Acoustic Absorption and Insulation

The superior acoustic absorption in the low-to-medium frequency range (1000 - 4000 Hz) is driven by a synergistic effect of two distinct mechanisms. While the increased specific surface area and tortuosity enhance visco-thermal dissipation (friction between sound waves and fibers), the primary mechanism at these frequencies is typically membrane resonance. Under acoustic excitation, the entire hierarchical nanofiber web vibrates, efficiently converting acoustic energy into kinetic and thermal energy. The intricate pore structure of PET nanofiber mats effectively dissipates sound waves, particularly in the low-to-medium frequency range (1000 - 4000 Hz), where conventional materials often fail (**Figure 7**) [21].

### 5.2. Antibacterial and Functional Textiles

The solvent-free nature of A-MCES makes it an ideal platform for fabricating functionalized textiles without the risk of solvent toxicity or leaching. Antibacterial agents, such as metal oxide nanoparticles, can be directly compounded into

the polymer melt prior to spinning. Tsang, A. C. H. *et al.* successfully fabricated recycled PET (r-PET) fibers functionalized with Zinc Oxide (ZnO) nanoparticles. Their study demonstrated that these melt-processed composite fibers exhibited significant inhibition zones against *E. coli* and *S. aureus* (Figure 8). This approach not only valorizes recycled plastic but also produces durable, hygiene-grade textiles suitable for medical gowns and hospital bedding [22].

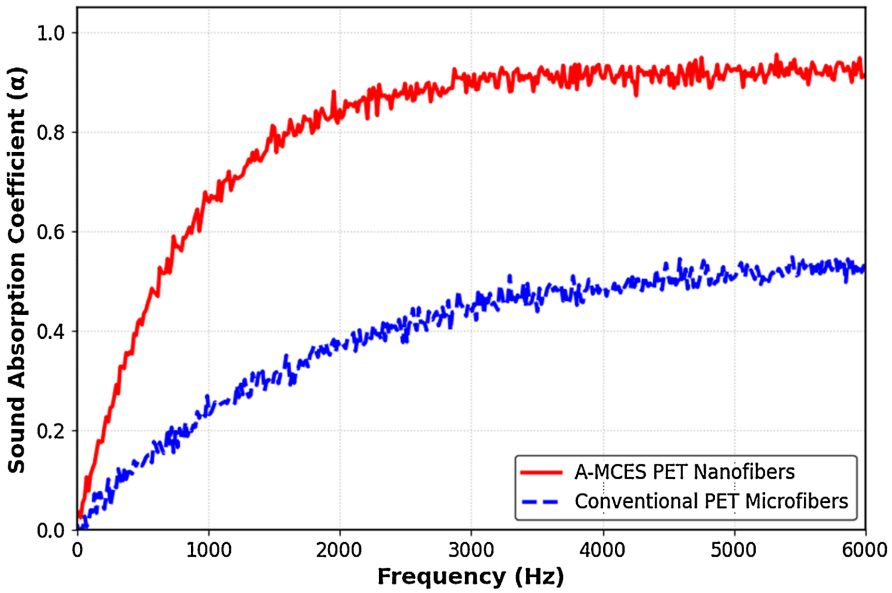


Figure 7. Acoustic absorption coefficient vs. Frequency. A-MCES nanofibers (red line) show superior absorption in the medium-frequency range compared to conventional microfibers (blue line). (Based on Gao, Y. *et al.* [21]).

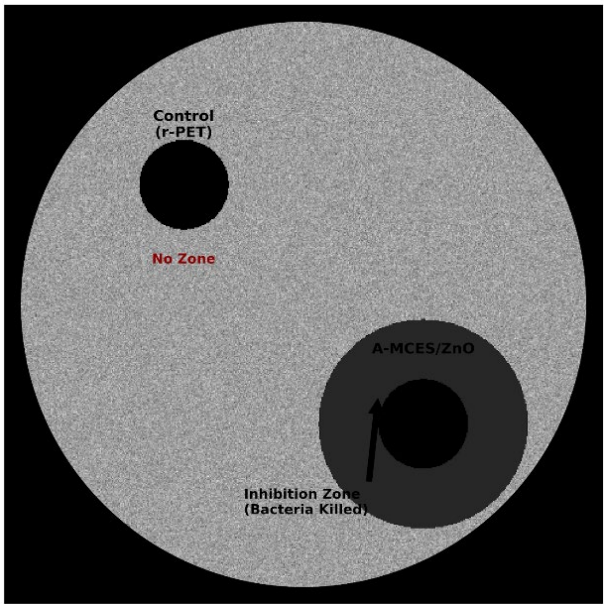


Figure 8. Antibacterial activity (Inhibition Zone Test). The A-MCES/ZnO composite sample (bottom right) shows a distinct inhibition zone, whereas the control r-PET sample (top left) does not. (Based on Tsang, A. C. H. *et al.* [22]).

### 5.3. Energy Storage: Battery Separators

In the field of Lithium-Ion Batteries (LIBs), the separator is a critical component for safety and efficiency. Commercial polyolefin separators (PP/PE) suffer from poor thermal stability, leading to shrinkage at high temperatures and potential short circuits. PET, with its high melting point (~255˚C), offers superior thermal safety. Zander, N. E. *et al.* explored the production of recycled PET fibers via centrifugal melt spinning. They found that the resulting nonwoven mats possessed the necessary porosity and electrolyte uptake capability to function as high-performance separators. The A-MCES process, combining centrifugal force with electrostatic stretching, further refines the fiber diameter, potentially enhancing the ionic conductivity and charge-discharge performance of the batteries [23].

## 6. Conclusions and Future Perspectives

### 6.1. Conclusions

Air-Assisted Melt Centrifugal Electrospinning (A-MCES) has emerged as a transformative technology in the field of polymer processing, effectively bridging the critical gap between the high production efficiency of traditional melt spinning and the ultra-fine fiber capabilities of solution electrospinning. This review has systematically highlighted that the synergistic coupling of centrifugal inertia, electrostatic dispersion, and high-velocity aerodynamic shear offers a robust, solvent-free pathway for the mass production of PET micro/nanofibers, fundamentally addressing the environmental toxicity issues associated with solvent-based methods.

From a structural perspective, the transition from single-force to multi-force processing has revolutionized the morphological control of PET. By precisely regulating the airflow temperature and velocity, A-MCES successfully decouples the cooling rate from the strain rate. This unique ability promotes Stress-Induced Crystallization (SIC) within sub-micron fibers, yielding nonwovens that combine the superior mechanical strength of oriented engineering plastics with the high specific surface area of nanofiber mats. These attributes make A-MCES PET fibers exceptionally suitable for demanding applications in high-temperature filtration, environmental remediation, and biomedical scaffolds.

### 6.2. Future Perspectives

Despite the significant progress detailed in this review, several challenges must be addressed to facilitate the full-scale industrial adoption of A-MCES:

Energy Efficiency Optimization: The generation and maintenance of high-velocity hot airflow currently consume substantial energy, affecting the cost-effectiveness of the process. Future equipment design should focus on optimizing nozzle geometries (e.g., advanced Laval nozzles) to maximize drag force efficiency while minimizing compressed air and heat consumption.

Uniformity and Process Control: While throughput is high, the chaotic nature of whipping instability in a turbulent airflow field often leads to broader fiber diameter distributions compared to solution electrospinning. The integration of

real-time monitoring systems and closed-loop control algorithms will be essential to enhance batch-to-batch consistency and reduce structural defects. Pushing the Nanoscale Limit: Consistently producing PET fibers below the 100 nm scale via melt processing remains a physical hurdle due to high melt viscosity. Future research directions may involve the development of benign plasticizers or eutectic solvent additives that can temporarily lower viscosity during spinning without compromising the biocompatibility or mechanical integrity of the final product. While A-MCES requires substantial thermodynamic energy input to generate compressed supersonic airflow and maintain high melt temperatures, this must be weighed qualitatively against the massive energy sinks and environmental costs associated with solvent distillation, recovery, and remediation inherent to traditional solution electrospinning.

In summary, A-MCES represents a cornerstone of "Green Manufacturing" in the fiber industry. With continued advancements in thermodynamic control and equipment engineering, it is poised to become the dominant technology for the sustainable production of high-performance functional nonwovens.

## Conflicts of Interest

The authors declare no conflicts of interest regarding the publication of this paper.

## References

[1] Li, D. and Xia, Y. (2004) Electrospinning of Nanofibers: Reinventing the Wheel? *Advanced Materials*, **16**, 1151-1170. https://doi.org/10.1002/adma.200400719

[2] Huang, Z., Zhang, Y., Kotaki, M. and Ramakrishna, S. (2003) A Review on Polymer Nanofibers by Electrospinning and Their Applications in Nanocomposites. *Composites Science and Technology*, **63**, 2223-2253. https://doi.org/10.1016/s0266-3538(03)00178-7

[3] Lyons, J., Li, C. and Ko, F. (2004) Melt-Electrospinning Part I: Processing Parameters and Geometric Properties. *Polymer*, **45**, 7597-7603. https://doi.org/10.1016/j.polymer.2004.08.071

[4] Liu, Y., Tan, J., Yu, S., Yousefzadeh, M., Lyu, T., Jiao, Z., *et al.* (2020) High-Efficiency Preparation of Polypropylene Nanofiber by Melt Differential Centrifugal Electrospinning. *Journal of Applied Polymer Science*, **137**, Article No. 48299. https://doi.org/10.1002/app.48299

[5] Zhmayev, E., Cho, D. and Joo, Y.L. (2010) Nanofibers from Gas-Assisted Polymer Melt Electrospinning. *Polymer*, **51**, 4140-4144. https://doi.org/10.1016/j.polymer.2010.06.058

[6] Dupaix, R.B. and Boyce, M.C. (2005) Finite Strain Behavior of Poly(ethylene Terephthalate) (PET) and Poly(ethylene Terephthalate)-Glycol (PETG). *Polymer*, **46**, 4827-4838. https://doi.org/10.1016/j.polymer.2005.03.083

[7] Sarkar, K., Gomez, C., Zambrano, S., Ramirez, M., de Hoyos, E., Vasquez, H., *et al.* (2010) Electrospinning to Forcespinning™. *Materials Today*, **13**, 12-14. https://doi.org/10.1016/s1369-7021(10)70199-1

[8] Jin, M., *et al.* (2023) Influence of a Meltblown Die with a Laval Airstream Channel on the Manufacturing Process of a Polymer Fiber Based on an Orthogonal Test and Simulation Analysis. *ACS Omega*, **8**, 47746-47759.

[9] Li, Y., Yin, X., Yu, J. and Ding, B. (2019) Electrospun Nanofibers for High-Performance Air Filtration. *Composites Communications*, **15**, 6-19. https://doi.org/10.1016/j.coco.2019.06.003

[10] Hutmacher, D.W. and Dalton, P.D. (2011) Melt Electrospinning. *Chemistry—An Asian Journal*, **6**, 44-56. https://doi.org/10.1002/asia.201000436

[11] Zander, N.E., Sweetser, D., Cole, D.P. and Gillan, M. (2015) Formation of Nanofibers from Pure and Mixed Waste Streams Using Electrospinning. *Industrial & Engineering Chemistry Research*, **54**, 9057-9063. https://doi.org/10.1021/acs.iecr.5b02279

[12] Awaja, F. and Pavel, D. (2005) Recycling of PET. *European Polymer Journal*, **41**, 1453-1477. https://doi.org/10.1016/j.eurpolymj.2005.02.005

[13] Dalton, P.D., Grafahrend, D., Klinkhammer, K., Klee, D. and Möller, M. (2007) Electrospinning of Polymer Melts: Phenomenological Observations. *Polymer*, **48**, 6823-6833. https://doi.org/10.1016/j.polymer.2007.09.037

[14] Greiner, A. and Wendorff, J.H. (2007) Electrospinning: A Fascinating Method for the Preparation of Ultrathin Fibers. *Angewandte Chemie International Edition*, **46**, 5670-5703. https://doi.org/10.1002/anie.200604646

[15] Liu, C., Hsu, P., Lee, H., Ye, M., Zheng, G., Liu, N., *et al.* (2015) Transparent Air Filter for High-Efficiency $PM_{2.5}$ Capture. *Nature Communications*, **6**, Artcle No. 6205. https://doi.org/10.1038/ncomms7205

[16] Reneker, D.H. and Yarin, A.L. (2008) Electrospinning Jets and Polymer Nanofibers. *Polymer*, **49**, 2387-2425. https://doi.org/10.1016/j.polymer.2008.02.002

[17] Forestier, E., Combeaud, C., Guigo, N., Sbirrazzuoli, N. and Billon, N. (2020) Understanding of Strain-Induced Crystallization Developments Scenarios for Polyesters: Comparison of Poly(ethylene Furanoate), PEF, and Poly(ethylene Terephthalate), PET. *Polymer*, **203**, Article ID: 122755. https://doi.org/10.1016/j.polymer.2020.122755

[18] Perret, E. and Hufenus, R. (2021) Insights into Strain-Induced Solid Mesophases in Melt-Spun Polymer Fibers. *Polymer*, **229**, Article ID: 124010. https://doi.org/10.1016/j.polymer.2021.124010

[19] Xue, J., Wu, T., Dai, Y. and Xia, Y. (2019) Electrospinning and Electrospun Nanofibers: Methods, Materials, and Applications. *Chemical Reviews*, **119**, 5298-5415. https://doi.org/10.1021/acs.chemrev.8b00593

[20] Puguan, J.M.C., Pornea, A.G.M., Ruello, J.L.A. and Kim, H. (2022) Double-Porous PET Waste-Derived Nanofibrous Aerogel for Effective Broadband Acoustic Absorption and Transmission. *ACS Applied Polymer Materials*, **4**, 2626-2635. https://doi.org/10.1021/acsapm.1c01918

[21] Gao, Y. and Cranston, R. (2008) Recent Advances in Antimicrobial Treatments of Textiles. *Textile Research Journal*, **78**, 60-72. https://doi.org/10.1177/0040517507082332

[22] Tsang, A.C.H., Wong, M.Y.L., Tsang, C., Suen, D.W. and Lu, X. (2025) Development of ALN-Loaded PET Separators from Waste Water Bottle Plastics with Superior Thermal Characteristics for Next-Generation Lithium-Ion Batteries. *RSC Advances*, **15**, 5452-5461. https://doi.org/10.1039/d4ra06478j

[23] Zander, N.E., Gillan, M. and Sweetser, D. (2016) Recycled PET Nanofibers for Water Filtration Applications. *Materials*, **9**, Article No. 247. https://doi.org/10.3390/ma9040247